Specific contact resistivity of nanowire devices

E. Stern,[a] G. Cheng,[b] M. P. Young, and M. A. Reed
Departments of Electrical Engineering, Biomedical Engineering, and Applied Physics, Yale University, P.O. Box 208284, New Haven, Connecticut 06520

(Received 8 September 2005; accepted 20 November 2005; published online 30 January 2006)

We present a study of specific contact resistivity from multiterminal Kelvin measurements for GaN nanowire (NW) devices. Nanowire specific contact resistivity is found to be process-independent and in good agreement to that of epitaxially grown GaN. A strong dependence of NW specific contact resistivity on carrier density is observed to be in good agreement with theory. © *2006 American Institute of Physics*. [DOI: 10.1063/1.2163454]

GaN nanowires (NWs) are a subject of great interest because they hold the potential for nano-optoelectronic devices due to their blue photoluminescence[1–4] and because Mg has been successfully incorporated as a *p*-type dopant,[5] thus in-wire *p-n* junctions can be fabricated.[6] There have been many reports of high-quality GaN NWs grown by a variety of methods, including laser ablation[7,8] and hot-wall chemical vapor deposition (CVD) with metallorganic[9,10] and solid sources.[6,11] These studies use either Ti/Au or Ni/Au metallizations to define contacts to the NWs because these schemes have been shown to make successful low-resistivity contacts to epitaxially grown GaN and GaN NWs.[6,12,13] In order to successfully characterize and eventually optimize device performance it is important to control specific contact resistivity; in this Letter we report a study of specific contact resistivity for NW devices.

A Ni/Au metallization was chosen to contact the NWs because this scheme has previously been seen to produce Ohmic contacts to degenerately doped NWs.[14] The NWs were grown in a hot-wall tube furnace by CVD and have been shown to be single-crystal hexagonal wurtzite.[11] The growth conditions of the wires used in this paper are described in Table I. Nanowires from Growth A were used for the e-beam devices; NWs from Growths B through D produced optical four-point devices. Previous studies have shown devices from these latter three growths had similar electrical characteristics.[11]

Devices were fabricated by transferring the NWs to a Si/SiO_2 wafer followed by liftoff metallization of 50 nm Ni/200 nm Au with patterns defined either by electron-beam (e-beam) or optical lithography.[14] Devices processed by e-beam lithography were annealed at 475 °C after fabrication and those processed with optical lithography were subjected to an oxygen plasma prior to metallization but were not annealed.[14] Leads yielding NW devices were imaged with a field emission scanning electron microscope (FE-SEM) and lead pairs contacting multiple NWs were discarded. The length and diameter of all devices were determined from FE-SEM images; lengths were measured to the nearest 50 nanometers and diameters were assessed to the nearest five nanometers. Four-terminal Kelvin probe measurements were taken by sweeping a current (I_4) across the outer leads and measuring the voltage (V_4) across the inner leads. Device resistances are defined as the zero-bias slope of the inverse of the $I_4(V_4)$ dependence. The NW resistivity is defined conventionally as

$$\rho_{NW} = R_4 \frac{A_{NW}}{L}, \quad (1)$$

where A_{NW} is the cross-sectional NW area and L is the source-drain NW length.

All samples measured had a linear best-fit correlation coefficient $R^2 > 0.995$. The contact resistance, R_C, of a device is determined by subtracting the four-point resistance from the two-point value from the inner electrodes of the four-point contact. The specific contact resistivity is then defined as

$$\rho_C = R_C A_C, \quad (2)$$

where A_C is the area of the contact, which is assumed to be half of the total NW surface area lying under the metal lead (reasonable for e-beam evaporated films). Figure 1 depicts a typical device used in this study, where the conformality of the metallization to the top surface of the NW, for which we assume a circular cross section, is evident.

Representative two-point and four-point $I(V)$ curves are shown in Fig. 2 for an optically and an e-beam-processed device. In addition to the Ohmic nature of the contacts, it is seen that the current levels of the two-point and four-point measurements are nearly identical, suggesting low specific contact resistivities.

The measured specific contact resistivity of 32 optical and six e-beam devices are plotted versus NW resistivity in Fig. 3. The linear best-fit line indicates the same functional dependence $\rho_C(\rho_{NW})$, independent of processing method (the average higher ρ_{NW} values observed for e-beam fabricated devices are due to run-to-run growth variations). The NW specific contact resistivity is also comparable to that of an

TABLE I. Table showing the growth conditions varied for GaN NW samples used in this study. For all samples, the catalyst was Ni, the Pressure was ~760 Torr, the NH_3 flux was 100 sccm, and the gallium source was a mixture of elemental gallium and gallium oxide.

Growth	Substrate	Temp (°C)
A	Alumina	840
B	Silicon	900
C	Silicon	1000
D	Silicon	1100

[a]Author to whom correspondence should be addressed; electronic mail: guosheng.cheng@yale.edu
[b]Electronic mail: eric.stern@yale.edu

 © 2006 American Institute of Physics
Downloaded 30 Jan 2006 to 128.36.14.23. Redistribution subject to AIP license or copyright, see http://apl.aip.org/apl/copyright.jsp

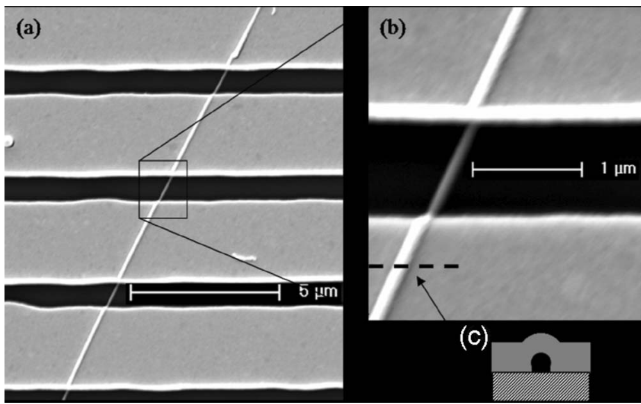

FIG. 1. (a) FE-SEM image at 5000× of a typical four-point contact to a NW. (b) FE-SEM image at 20 000× of the middle contacts of the same device. It can be seen that the metal conformally covers the top of the NW. (c) Cross-section schematic shown by the dotted black line in (b) depicting the metal-NW interface as half the NW surface area.

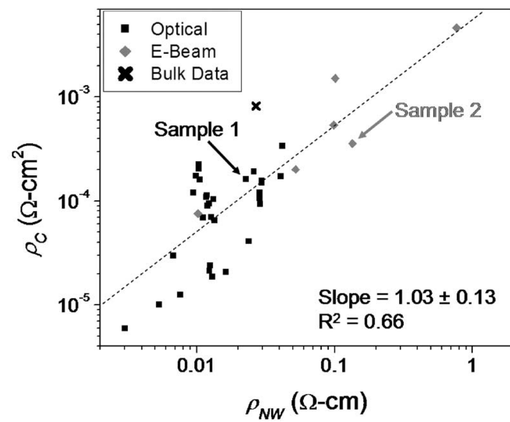

FIG. 3. Scatter plot of contact vs NW resistivity including the bulk datapoint from Ref. 12. The devices highlighted by arrows, Samples 1 and 2, are the devices from Fig. 2. A linear best-fit to the NW data is shown as a dotted line.

unannealed contact to bulk n-GaN, which for $\rho \sim 0.027$ Ω-cm (from Ref. 12 with 1.5×10^{19} cm^{-3} and using the same carrier density-resistivity relation as for NW samples) has $\rho_C = 8.2\times10^{-4}$ Ω-cm^2, and is plotted in Fig. 4.

To understand the nature of the Ohmic contacts, the dependence of ρ_C on the carrier density, n, was studied. Samples were prepared with backgates and $I_{SD}(V_{SD})$ measurements were taken while varying V_{GD} from −20 to 20 V. The transconductance was calculated from the slope of a linear best-fit to the $I_{SD}-V_{GD}$ for $V_{SD}=1$ V. The carrier concentration was then calculated according to

$$n = \frac{\sigma}{e\mu}, \tag{3}$$

where

$$\mu = \left(\frac{C}{L^2}V_{SD}\right)^{-1} \left.\frac{\partial I_{SD}}{\partial V_{GD}}\right|_{V_{SD}=1}, \tag{4}$$

with $C = 2\pi\varepsilon\varepsilon_0 L/\ln(4h/d)$, where L is the source-drain NW length, h is the SiO_2 thickness, and d is the NW diameter.

The specific contact resistivity is plotted against the carrier concentration in Fig. 4. The values of n range from 4.27×10^{19} to 1.47×10^{20} cm^{-3}. The specific contact resistivity for degenerate samples is related to donor density according to

$$\rho_C \propto e^{B\phi_B/\sqrt{N}}, \tag{5}$$

where $B = (4\pi/h)\sqrt{\varepsilon m^*}$, h is Planck's constant, ε is the dielectric permittivity, and m^* is the effective mass of the electron.[15] Since for NWs, $N_D \gg N_A$ it can be assumed that $n \propto N$ so Eq. (6) can be used to fit the data in Fig. 4 ($\varepsilon/\varepsilon_0|_{\mathrm{GaN}} = 8.9$,[16] $\phi_B = 1.11$,[13,17] and $m^* = 0.20m_0$[16]). The solid gray line in Fig. 4 shows this theoretical fit, in reasonable agreement with a linear least-squares fit (broken black line) to the experimental data.

This work shows that metal contacts to degenerate semiconducting NWs give comparable experimental data and can be treated with the same tunneling model as for bulk material. The NW specific contact resistivities reported here should be considered an upper bound and open to improvement; bulk specific contact resistivities as low as 8.9×10^{-8} Ω-cm^2 have been reported[18] by very high temperature annealing conditions not attempted in this study.

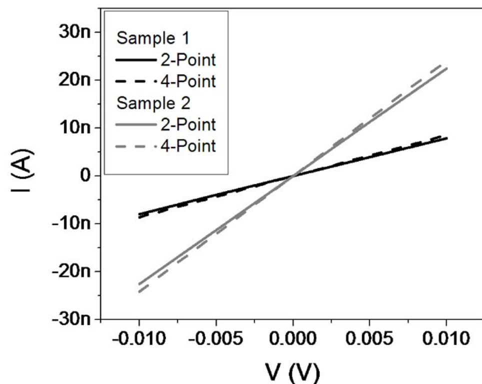

FIG. 2. Two-point and four-point $I(V)$ curves for an e-beam processed NW (Sample 1) and an opticall processed NW (Sample 2). The two-point curve was taken by varying the voltage and measuring current. The four-point curve was taken by varying the current while measuring voltage, and inverting.

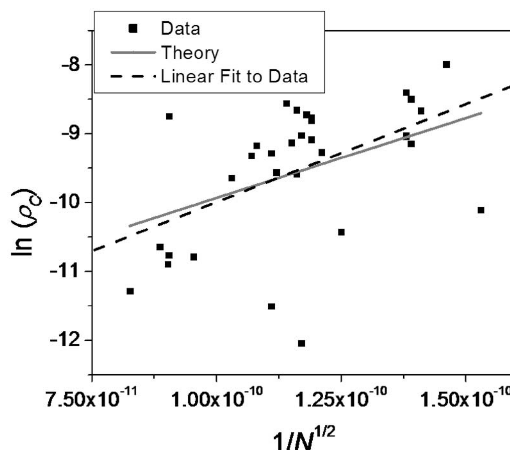

FIG. 4. Plot of $\ln(\rho_C)$ vs $1/N^{1/2}$ for 32 optically defined devices with backgates. The broken black line is a linear best-fit through the data with a slope of $2.84\pm0.88\times10^{10}$, an intercept of -12.84 ± 1.04, and $R^2=0.26$. The solid gray line shows the theoretic fit, with a slope of 2.32×10^{10} and an intercept of −12.25.

Downloaded 30 Jan 2006 to 128.36.14.23. Redistribution subject to AIP license or copyright, see http://apl.aip.org/apl/copyright.jsp

The authors would like to thank Dr. James Klemic, Professor Jung Han, and Dr. James Hyland for many helpful discussions, Daniel Turner-Evans and Elizabeth Broomfield for help with data manipulation, Dr. Elena Cimpoiasu, Ryan Munden, and Aric Sanders for aiding with the measurement setup, Dr. Zhenting Jiang for help with the FE-SEM microscopy work. This work was partially supported by DARPA through AFOSR, ARO (DAAD19-01-1-0592), AFOSR (F49620-01-1-0358), NASA (NCC 2-1363), by a Department of Homeland Security graduate fellowship, and by a NSF graduate fellowship.

[1]J. Goldberger, R. He, Y. Zhang, S. Lee, H. Yan, H.-J. Choi, and P. Yang, Nature (London) **422**, 599 (2003).
[2]J. C. Johnson, H. J. Choi, K. P. Knutsen, R. D. Schaller, P. Yang, and R. J. Saykally, Nat. Mater. **1**, 106 (2003).
[3]S. Nakamura, Science **281**, 956 (1998).
[4]H. W. Seo, S. Y. Bae, J. Park, H. Yang, K. S. Park, and S. Kim, J. Chem. Phys. **116**, 9492 (2002).
[5]Z. H. Zhong, F. Qian, D. L. Wang, and C. M. Lieber, Nano Lett. **3**, 343 (2003).
[6]G. Cheng, Z. Kolmakov, Y. Zhang, M. Moskovitz, R. Munden, M. A. Reed, G. Wang, D. Moses, and J. Zhang, Appl. Phys. Lett. **83**, 1678 (2003).
[7]M. Kim, B.-H. Jeon, J.-Y. Kim, and J.-H. Choi, Synth. Met. **135**, 743 (2003).
[8]X. F. Duan and C. M. Lieber, J. Am. Chem. Soc. **122**, 188 (2000).
[9]E. A. Stach, P. J. Pauzauskie, T. Kuykendall, J. Goldberger, R. R. He, and P. D. Yang, Nano Lett. **3**, 867 (2003).
[10]M. Law, J. Goldberg, and P. D. Yang, Annu. Rev. Mater. Res. **34**, 83 (2004).
[11]E. Stern, G. Cheng, E. Cimpoiasu, R. Klie, S. Guthrie, J. Klemic, I. Kretzschmar, E. Steinlauf, D. Turner-Evans, E. Broomfield, J. Hyland, R. Koudelka, T. Boone, M. Young, A. Sanders, R. Munden, T. Lee, D. Routenberg, and M. A. Reed (in press).
[12]S. Pal and T. Sugino, Appl. Surf. Sci. **161**, 263 (2000).
[13]J. S. Hwang, D. Ahn, S. H. Hong, H. K. Kim, S. W. Hwang, B. H. Jeon, and J. H. Choi, Appl. Phys. Lett. **85**, 1636 (2004), who studied the effects of varying the thickness of Ti for Ti/Au contacts on GaN NW resistances but could not extract specific contact resistivities.
[14]E. Stern, G. Cheng, C. Li, J. Klemic, C. Zhou, and M. A. Reed (in press).
[15]W. R. Runyan and K. E. Bean, *Semiconductor Integrated Circuit Processing Technology* (Addison-Wesley, New York, 1990), pp. 520–528.
[16]V. Bougrov, M. E. Levinshtein, S. L. Rumyantsev, and A. Zubrilov, in *Properties of Advanced SemiconductorMaterials GaN, AlN, InN, BN, SiC, SiGe*, edited by M. E. Levinshtein, S. L. Rumyantsev, and M. S. Shur, (Wiley, New York, 2001), pp. 1–30.
[17]S. M. Sze, *Physics of Semiconductor Devices*, 2nd ed. (Wiley, New York, 1981), p. 251.
[18]Z. Fan, S. N. Mohammad, X. Kim, O. Aktas, A. E. Botchkarev, and H. Morkoc, Appl. Phys. Lett. **80**, 3548 (1996).

Downloaded 30 Jan 2006 to 128.36.14.23. Redistribution subject to AIP license or copyright, see http://apl.aip.org/apl/copyright.jsp